

Interacting Circular Nanomagnets

A. A. Fraerman, S. A. Gusev, L. A. Mazo, I. M. Nefedov, Yu. N. Nozdrin, I. R. Karetnikova, M. V. Sapozhnikov, I. A. Shereshevsky,
L. V. Suhodoev

Russian Academy of Science

Institute for Physics of Microstructures

GSP-105, Nizhny Novgorod, 603600, Russia

E-mail: msap@ipm.sci-nnov.ru

Abstract

Regular 2D rectangular lattices of permalloy nanoparticles (40 nm in diameter) were prepared by the method of the electron lithography. The magnetization curves were studied by Hall magnetometry with the compensation technique for different external field orientations at 4.2K and 77K. The shape of hysteresis curves indicates that there is magnetostatic interaction between the particles. The main peculiarity is the existence of remanent magnetization perpendicular to easy plain. By numerical simulation it is shown, that the character of the magnetization reversal is a result of the interplay of the interparticle interaction and the magnetization distribution within the particles (vortex or uniform).

PACS: 75.60.Jp

1 Introduction

There is a great interest to magnetic nanoparticles nowadays. The attention is focused on the single-particle magnetization state. Now it is well known that competition between the magnetostatic and exchange energy in a very small (~ 20 nm) particle leads to a single - domain state. If the radius of the particle is sufficiently large, nonuniform distribution of magnetization has minimal energy. In isotropic magnetic particle it is a vortex. That particle was referred to as circular nanomagnet [1]. Nowadays such vortex distribution of magnetization in nanomagnets is under detailed investigation [2]. Such systems are considered as very perspective for use in RAM (Random Access Memory) devices [3]. It was obvious that distribution of magnetization in nanomagnets must depend on interaction between them. One fundamental type of interaction, which can lead to collective behavior, is the magnetostatic interaction. On the other hand, the character of the interaction itself is determined by the magnetization state of the particle. In our work we experimentally investigate magnetization curves of regular lattices of Ni_3Fe nanoparticles for different external field orientations. As the result it is demonstrated that in the case of the anisotropic (rectangular) lattice the magnetization distribution within individual particle during magnetization reversal process depends on the external field orientation to the lattice axis. It is a consequence of the interplay of the interparticle interaction and single particle state. Particles can be both at single-domain and vortex state at zero field. The appearance of the magnetization vortices leads to appearance of the remanent magnetization while magnetizing perpendicular to the system easy axis. The occurrence of such effect was explained on the basis of the model of two magnetostatically interacted nanomagnets.

2 Experiment

Arrays of magnetic particles were fabricated by improved electron-beam lithography. The main feature of our creation method is the usage of fullerene as the resist for electron lithography. The smaller size of C_{60} molecules and the ability of fullerene to modify their physical and chemical properties under exposure of electrons promise good perspectives at use this new material for high-resolution nanofabrication. Recently capabilities of C_{60} as negative e-resist have been demonstrated to fabrication of 20-30 nm Si pillars [4]. The main steps of the procedure for manufacture permalloy nanoparticles are thin films deposition, exposure by e-beam, development and two-stage etching. We have used double-layer mask containing the C_{60} film as a sensitive layer and Ti film as a transmitting layer. Permalloy and Ti films have been prepared by pulse laser evaporation on the substrate at room temperature. Fullerene films were deposited by sublimating of a C_{60} powder at temperature 350 C in vertical reactor with hot walls and supplied with cooling holder for the substrate. Transmission electron microscopy, selected area diffraction and X-ray diffraction of metals and fullerene films were carried out to check crystalline structure and thickness of layers. Maximum dimensions of metals crystallites not exceeded 5 nm, C_{60} films had an almost amorphous structure. The thickness of magnetic layers was varied from 25 to 45 nm. The thickness of masking films was 20 nm for the C_{60} layer and 30 nm for Ti film. The fullerene was patterned in the JEM-2000EX electron microscope with scanning electron microscopy (SEM) mode by 200 kV e-beam, which diameter is possible to change from 10 nm and over. Utilizing the high-energy electron beam decreases the amount of backscattering electrons and the shape of patterns becomes defined better. Usually the doses for practical usage were 0.05-0.1 C/cm^2 , because it assured the reproducibility and uniformity of patterns sizes. Electron beam irra-

diation of C_{60} films reduces the solvability of fullerene in organic solvents. The most likely reasons of changes of the solvability are electron induced polymerization C_{60} molecules accompanied partially graphitization ones [4, 5]. Exposed samples were developed in the toluene during 1 min and then patterns were transferred into the Ti layer by plasma etching with CF_2Cl_2 atmosphere. The last step of fabrication the magnetic particles is the Ar^+ ion milling of Ni_3Fe films, using this double-layered mask. Basically, resistance of C_{60} films to the ion milling is sufficient to use this single mask with little bit greater thickness, but multiple etch steps are necessary to ensure a uniformity and reproducibility of the sizes of particles. By carefully monitoring the elemental composition of samples by means EDS (energy dispersion spectroscopy) qualitative microanalysis and checking up the morphology of particles by SEM we can better detect the end points of plasma etching and ion milling processes. However, usually we have done some overmilling at the last step, to prevent presence any magnetic substance between the particles we make. One of SEM images of arrays of ferromagnetic particles is present at Fig.1. The shape of ferromagnetic particles is a disc, which thickness equals the thickness of initial permalloy film.

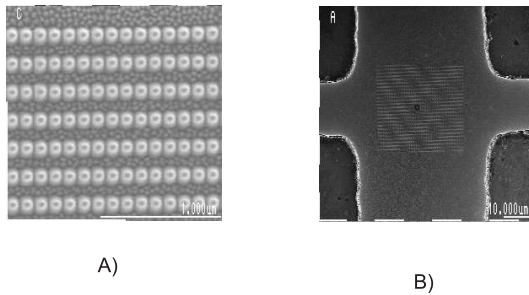


Figure 1: The SEM-image of the sample 1 (See the table 1). A) The lattice of the 40-50 nm particles is visible with the background of the 10 nm roughnesses of the sublayer. B) Sample position in the Hall cross.

The parameters of the investigated samples are summarized in the Table below.

There a and b are the lattice parameters, h is the high of the particles and d is their diameter. The total number of the particles is equal to 10^5 .

N	a(nm)	b(nm)	h(nm)	d(nm)
1	90	180	45	50
2	120	240	25	80

To provide measurements of the magnetic properties we choose a Hall microsensor technique. Recently it was shown that Hall magnetometer is a very powerful tool for investigation of magnetic properties of 2D nanoparticles lattices [6].. In our work we successfully applied commercial magnetometer based on the Hall response in a semiconductor (InSb) to investigation into the cooperative behavior of artificially fabricated 2D permalloy nanoparticle array. The widths of the current and the voltage probes are $100\mu\text{m}$ and $50\mu\text{m}$ and the thickness of the semiconductor layer is $10\mu\text{m}$. The lattice of the particles was produced in the active area of one of the Hall crosses. The difference in the Hall voltage between this sample cross and the closely spaced reference is measured using the bridge circuit [6]. If the bridge is properly balanced, the resulting output voltage is proportional to the sample contribution to the magnetic induction. This contribution can then be calculated so that $\Delta B = V/RI$ where R is the Hall coefficient and I is the measured current. Typically we use the dc current of 50 mA. The large Hall response in the combination with the good coupling of the small samples to the device results in the excellent spin sensitivity (ratio signal/noise is approximately 100). The sensor works over a large

range of the magnetic field and temperature. We investigate the magnetic properties of the samples by measuring the perpendicular magnetization as a function of the direction and magnitude of the applied field. As the used method allows to measure only the B_z -component, we provide our investigation with the three orientation of the external magnetic field: 1) the field is perpendicular to the sample plane ($\theta = 0^\circ$); 2) the field is directed at 45 deg. to the sample plane along the short side of the rectangle cell ($\theta = 45^\circ, \phi = 0^\circ$); 3) the field is directed at 45 deg. to the sample plane along the long side of the rectangle cell ($\theta = 45^\circ, \phi = 90^\circ$). The results of this measurements for $T = 4.2K$ are represented on the Figs. 2, 3, 4

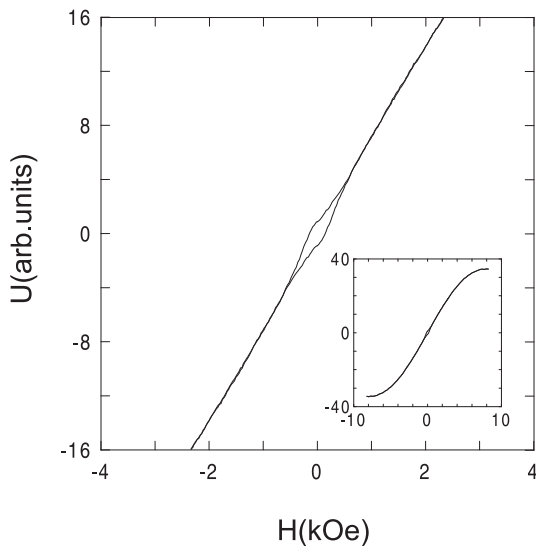


Figure 2: The dependence of Hall signal on the magnetic field with $\theta = 0^\circ$. The whole magnetization curve is shown on the casing-in.

accordingly. The difference in the magnetization curves indicates the collective behavior of the system, which is the result of the magnetostatic interaction between particles. The hysteresis if the field directed at $\theta = 45^\circ, \phi = 0^\circ$ (Fig. 3) is the attribute of the easy axis of the magnetization which is directed along the short side of the rectangle cell. The remanent magnetization is absent in this case. The

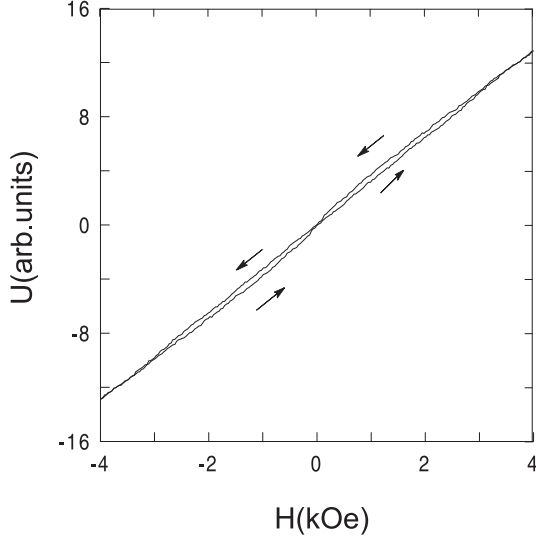


Figure 3: The dependence of Hall signal on the magnetic field with $\theta = 45^\circ$, $\phi = 0^\circ$.

existence of such anisotropy in the dipole system was theoretically predicted [7, 8]. The magnetization curves if the field directed at $\theta = 0^\circ$ or $\theta = 45^\circ$, $\phi = 90^\circ$ (Figs. 2, 4) are qualitatively similar. They have hysteresis in the weak magnetic field with the remanent magnetization which is approximately 5 % of the saturation magnetization. The magnetization curves for the second sample is qualitatively similar those of the first sample, although the samples themselves has the difference shape of the particles. The particles have the polycrystal structure (this was determined by the X-ray diffraction) and do not have the anisotropy of the form in the plane of the system. In this case the difference of the magnetization curves for the different orientation of the external magnetic field to the structure lattice is a positive attribute of the collective behavior of the system.

The existence of the anisotropy axis in the plane of the sample with the rectangular lattice was predicted earlier [7, 8] and was principally expected. As for the hysteresis of the magnetization curves and the remanent magnetization for the sample with the rectangular lattice if the external magnetic field direction is $\theta = 0^\circ$ or

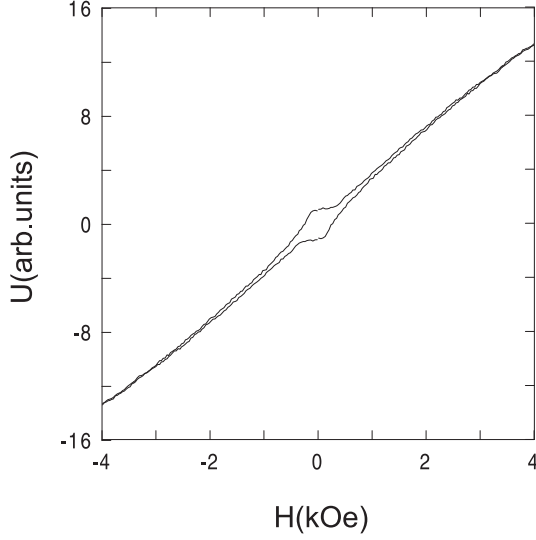


Figure 4: The dependence of Hall signal on the magnetic field with $\theta = 45^\circ$, $\phi = 90^\circ$.

$\theta = 45^\circ$, $\phi = 90^\circ$, their existence were unexpected. The effect can not be explained by the single particle properties. In this case the remanent magnetization must exist for the every direction of the magnetic field.

The first sample was investigated at $T=77K$ also. The hysteresis with the field directed at $\theta = 45^\circ$, $\phi = 0^\circ$ did not be observed. The hysteresis with the field directed at $\theta = 0^\circ$ or $\theta = 45^\circ$, $\phi = 90^\circ$ was qualitatively changed (Fig. 5).

We suppose that the observed behavior of the system is connected with the fact that the particles of the examined dimension can be in two states. First is a single domain state, the second is a state with magnetization distribution as a vortex. In this case the core of the vortex is magnetized perpendicularly. The interplay of the lattice anisotropy and the anisotropy of dipole interaction between particles leads to the following. The particles turn to be in the single domain state if the external field has the component directed along the particle chains. In this case the interaction within chain has the ferromagnetic character and therefore stabilizes the single domain state. On the other hand, if the system is demagnetized within

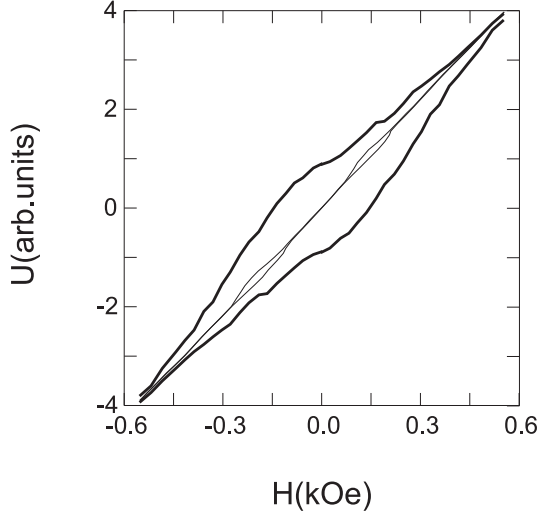


Figure 5: The changing of the magnetization curve hysteresis with the temperature: the thin line for $4.2^{\circ}K$, the thick one for $77^{\circ}K$. H is directed at $\theta = 0^{\circ}$.

the field perpendicular to the chains the dipole interaction has antiferromagnetic character within the chain and the particles turns to be in the vortex state. As core magnetization has its own coercivity, all cores are ferromagnetically ordered and the system has the remanent perpendicular magnetization. We perform numerical simulation to approve these suggestions.

3 Numerical simulation

Let us consider two magnetostatically interacting nanoparticles for simplicity. This model allows to investigate the magnetization distribution within particle in the anisotropic system with interaction. Really, due to fast dipole interaction decrease we may not to take into consideration the interaction between particles from different chains in the case of the 1:2 rectangular lattice. Let as consider the single particle of the appropriate sizes (radius is 50nm, height is 10-20nm) at first. The distribution of magnetization in such particle is driven by Landau-Lifshitz-Hilbert (LLH) equation

$$\frac{\partial \mathbf{M}}{\partial t} = -\frac{\gamma}{1 + \alpha^2} [\mathbf{M}, \mathbf{H}] - \frac{\alpha\gamma}{(1 + \alpha^2)M_s} [\mathbf{M}, [\mathbf{M}, \mathbf{H}]] \quad (1)$$

where γ is the gyromagnetic ratio, M_s is the saturation magnetization, α is the dimensionless damping parameter. The effective magnetic field $\mathbf{H}(\mathbf{r}, t)$ in (1) is a sum of several components, $\mathbf{H} = \mathbf{H}_0 + \mathbf{H}_d + \mathbf{H}_a + \mathbf{H}_e + \mathbf{H}_T$, where \mathbf{H}_0 is the applied external magnetic field, \mathbf{H}_d is the demagnetization field, \mathbf{H}_a is the field of anisotropy, \mathbf{H}_e is the exchange field within a particle and \mathbf{H}_T is the random field defined by the thermal fluctuations. To define the expression for magnetic field it is necessary to consider the energy of particle state as a functional of the magnetization distribution. Then the regular component of magnetic field is a variation derivative of the energy with respect to the magnetization. The energy functional is the sum of demagnetization, anisotropy and exchange energies, where

$$\begin{aligned} E_d(\mathbf{M}) &= -\frac{1}{2} \int_{V \times V} \text{div} \mathbf{M}(\mathbf{r}, t) \text{div} \mathbf{M}(\mathbf{r}', t) \frac{d\mathbf{r} d\mathbf{r}'}{|\mathbf{r} - \mathbf{r}'|} \quad (2) \\ &+ \int_{V \times \partial V} \text{div} \mathbf{M}(\mathbf{r}', t) (\mathbf{M}(\mathbf{r}, t), \mathbf{n}) \frac{d\mathbf{r} d\mathbf{r}'}{|\mathbf{r} - \mathbf{r}'|} - \frac{1}{2} \int_{\partial V \times \partial V} (\mathbf{M}(\mathbf{r}', t), \mathbf{n}') (\mathbf{M}(\mathbf{r}, t), \mathbf{n}) \frac{d\mathbf{r} d\mathbf{r}'}{|\mathbf{r} - \mathbf{r}'|} \\ E_a(\mathbf{M}) &= -\frac{K}{2} \int_V (\mathbf{M}(\mathbf{r}, t), \boldsymbol{\nu})^2 d\mathbf{r} \\ E_e(\mathbf{M}) &= -\frac{J}{2} \int_V |\nabla \mathbf{M}(\mathbf{r}, t)|^2 d\mathbf{r} \end{aligned}$$

$V, \partial V$ is the volume and surface of particle, \mathbf{n} is the unit vector of external normal to the surface at current point, $\mathbf{r} = (x, y, z)$ is space variable; K and $\boldsymbol{\nu}$ is the constant and direction of anisotropy; J is the constant of exchange interaction.

After discretization the corresponding expressions for magnetic field are:

$$H_d(\rho, t) = \frac{a^2}{h} \sum_{\rho'} (\hat{\mathbf{D}}^h(\rho - \rho') \mathbf{M}(\rho', t); \quad (3)$$

$$H_a(\rho, t) = K \sum_{\rho} (\mathbf{M}(\rho, t), \nu), \nu;$$

$$H_e(\rho, t) = \frac{J}{a^2} \sum_{\rho'} (\mathbf{M}(\rho, t) - \mathbf{M}(\rho', t))$$

Here $\hat{\mathbf{D}}^h$ is discrete analog of the dipole tensor, J and K is exchange and anisotropy constants, ν is the anisotropy axis vector, h is a particle thickness and a is the discretization scale. It is necessary to add the random component to the field to take into account the thermal fluctuations in the system. The field of thermal fluctuations is the "white noise" in space and time, i.e., the random Gauss function such that $\langle \mathbf{H}_T(\rho, t), \mathbf{H}_T(\rho', t') \rangle = \sigma^2(T) \delta_{\rho\rho'} \delta(t-t')$. The dependence of dispersion σ on temperature T is determined by the fluctuation-dissipation theorem,

$$\sigma^2(T) = \frac{2\alpha kT}{\gamma M_s a^2 h}. \quad (4)$$

The random field value depends on time step, and $H_T(\rho, t) = \frac{\sigma(T)}{\sqrt{(\Delta t)}} \xi(\rho, t)$, where $\xi(\rho, t)$ is a set of independent standard random Gauss three-dimensional vectors. Note that such an approach to solve stochastic LLH equation is well known and widely used in magnetic simulation [9, 10].

The explicit Euler method was used to solve the stochastic differential equation (1). The numerical scheme is represented in detail in other our article [11].

Let us now discuss some results of numerical experiments. First of all, for one cylindrical particle we find that the vortex magnetization state becomes ground state only when the height and radius of cylinder exceed some critical values. This fact was pointed out earlier in [12]. Up to the differences appearing due to the different particle shapes, our results are in good agreement with the ones presented in [12], and it is a good confirmation of the reasonability of our model. Fig. 6 demonstrates an example of vortex state in cylindrical particle of diameter 50nm and height 12.5nm ($a=1.25\text{nm}$, $\Delta t = 10^{-4}\text{ns}$) at zero external magnetic field. Note that such state has

nonzero z-component of magnetic moment. This can lead to appearance of hysteresis loop in z-magnetization curve in systems of magnetic particles.

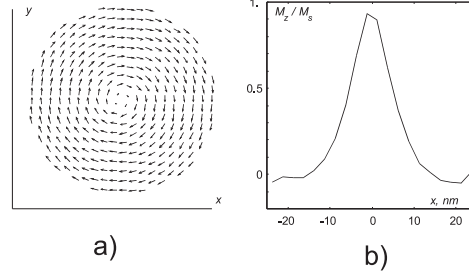


Figure 6: a) Vortex distribution of magnetization in cylindrical particle. b) z-component of magnetic moment versus x-coordinate.

If there are two interacting particles, magnetic hysteresis can change. Let x-axis be parallel to the line connecting the centers of particles. The goal is to investigate the dependence of z-magnetization curve on the direction of external magnetic field. Two different cases was considered: first, when the projection of external magnetic field on the (x, y) plane has only x-component, and second, when this projection has only y-component. In both cases the angle between the field and the z-axis is equal to 45° . Diameters of the particle are 50nm, height is 18nm, distance between the particle centers is 50nm ($a=1.25\text{nm}$, $\Delta t = 10^{-4}\text{ns}$). The corresponding z-magnetization curves are presented in Fig. 7. The hysteresis loop in the last curve (Fig. 7) is the result of vortex penetrating into the particles at some value of applied field. In contrast with this situation, the magnetization state remains quasi-homogeneous at all values of external field when its projection has only x-component, and as a consequence, the z-magnetization curve has no a hysteresis loop (Fig. 8).

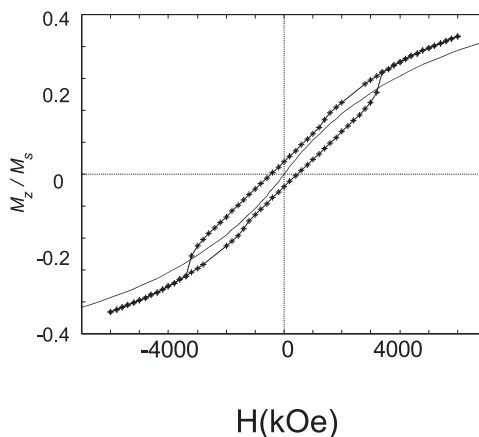


Figure 7: z-component of magnetization in two particles systems at $T=4\text{K}$, when external field is applied along a x-direction (solid line) and perpendicular to this direction (stars). Angle between external field and the z-axis is 45° .

4 Discussion

The fact suggests the following mechanism for the appearance of remanent magnetization with the external field orientation perpendicular to the particle chain. If the external magnetic field has component parallel to the particles axis, the magnetostatic interaction between particles decreases the total energy of the system and the remanent ($H = 0$) state is uniform. The perpendicular component of magnetic moment is absent as well as in experiment. In the case when the external magnetic field is perpendicular to the chains, magnetostatic interaction increases the total energy of the system. In order to decrease the magnetostatic interaction, distribution of the magnetic moment of the particle takes the vortex form. As discussed earlier, this vortex has a nonzero magnitude of remanent z - magnetization.

Besides there are fundamental changes in the magnetization curve of a rectangular unit cell sample occurring when the sample temperature is raised to 77K . It points to the fact that thermal fluctuations play a significant role in the system, as T_c of bulk permalloy is 885K . It is possible that this effect is determined by noise -

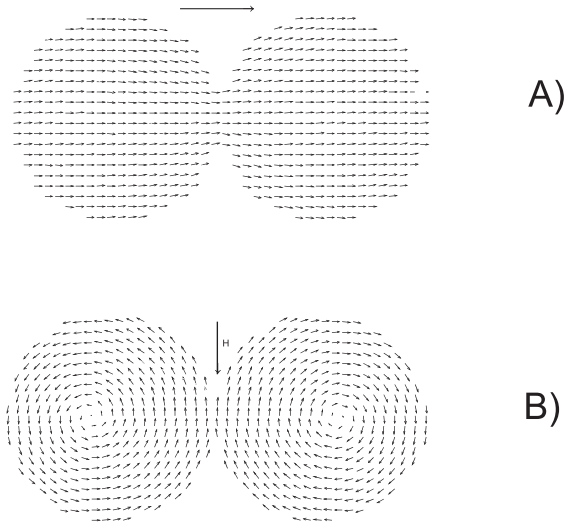


Figure 8: Uniform (A) and vortex (B) magnetization distribution in pair of the permalloy discs.

induced switching between vortex states with different polarization [13]. If the coercivity of the core become less than the antiferromagnetic magnetostatic interaction between cores the remanent magnetization on the system will be equal to zero. This hypothesis requires further theoretical investigation.

So it is shown that the interaction in the regular 2D rectangular lattice of nanoparticles can play a significant role. The interplay of anisotropy of magnetostatic interaction and lattice anisotropy determines the state the particles turns to be. It can be both vortex and single-domain state. Due to possibility of the vortex state existence, the system can have remanent magnetization directed perpendicularly to the system plane.

Acknowledgment.

We are grateful to Prof. A.S.Arrott for helpful discussion. The work was supported by the RFBR and PSSNS Program grants.

References

- [1] R.P.Cowburn, D.K.Koltsov, A.O.Adeyeye et al., Phys. Rev. Lett. **83**, 1042 (1999).
- [2] M.Schneider, H.Hoffmann, J.Zweck, Appl. Phys. Lett., **77**, 2909 (2000).
- [3] K.Bussmann et.al., J. Appl. Phys., **75**, 2476 (1999).
- [4] T.Tada and T.Kanayama, Jpn.J.Appl.Phys. **35**, L 63 (1996).
- [5] V.M.Mikushin, V.V.Shnitov, Sol.St.Phys., **39**, 187(1997) (in russian).
- [6] A. D.Kent et al. J.Appl.Phys. **67**, 6656 (1994).
- [7] V. M. Rosenbaum, Zh. Exp. Teor. Fiz., **99**, 1836 (1991) (in russian).
- [8] V. M. Rosenbaum, V. M. Ogenko, A. A. Chuiko, Uspekhi Fiz. Nauk, **161**, 79 (1991) (in russian).
- [9] R.P. Popko, L.L. Savchenko, N.V. Vorotnikov, Pis'ma JETP **69**, 555 (1999) (in russian).
- [10] E.D. Boerner, H.N. Bertran. IEEE Trans. on Magn. **33**, 3152 (1997).
- [11] to be published in Fiz.Tverd.Tela (in russian)
- [12] R.P. Cowburn, M.E. Welland. Appl, Phys. Lett. **72**, 2041 (1998).

[13] Y. Gaididei et al., Phys.Rev.B **59** 7010 (1999).